

AD-A149 424

AD

AD-E401 271

TECHNICAL REPORT ARLCD-TR-84022

**ELECTROMAGNETIC BRAKING OF A  
METALLIC PROJECTILE IN FLIGHT**

J. BENNETT  
T. GORA  
P. J. KEMMEY  
W. J. KOLKERT

DTIC  
ELECTE  
JAN 15 1985  
B

DECEMBER 1984



**U.S. ARMY ARMAMENT RESEARCH AND DEVELOPMENT CENTER**

**LARGE CALIBER WEAPON SYSTEMS LABORATORY**

**DOVER, NEW JERSEY**

**APPROVED FOR PUBLIC RELEASE; DISTRIBUTION UNLIMITED.**

DTIC FILE COPY

The views, opinions, and/or findings contained in this report are those of the author(s) and should not be construed as an official Department of the Army position, policy, or decision, unless so designated by other documentation.

Destroy this report when no longer needed. Do not return to the originator.

UNCLASSIFIED

SECURITY CLASSIFICATION OF THIS PAGE (When Data Entered)

REPORT DOCUMENTATION PAGE		READ INSTRUCTIONS BEFORE COMPLETING FORM
1. REPORT NUMBER Technical Report ARLCD-TR-84022	2. GOVT ACCESSION NO. AD-A149424	3. RECIPIENT'S CATALOG NUMBER
4. TITLE (and Subtitle) ELECTROMAGNETIC BRAKING OF A METALLIC PROJECTILE IN FLIGHT		5. TYPE OF REPORT & PERIOD COVERED 1 - 31 August 1983
		6. PERFORMING ORG. REPORT NUMBER
7. AUTHOR(s) J. Bennett                      W. J. Kolkert T. Gora P. J. Kenney		8. CONTRACT OR GRANT NUMBER(s)
9. PERFORMING ORGANIZATION NAME AND ADDRESS ARDC, LCWSL Applied Science Division (SMCAR-LCA-G) Dover, NJ 07801-5001		10. PROGRAM ELEMENT, PROJECT, TASK AREA & WORK UNIT NUMBERS
11. CONTROLLING OFFICE NAME AND ADDRESS ARDC, TSD STINFO Div (SMCAR-TSS) Dover, NJ 07801-5001		12. REPORT DATE December 1984
		13. NUMBER OF PAGES 18
14. MONITORING AGENCY NAME & ADDRESS (if different from Controlling Office)		15. SECURITY CLASS. (of this report) Unclassified
		15a. DECLASSIFICATION/DOWNGRADING SCHEDULE
16. DISTRIBUTION STATEMENT (of this Report)  Approved for public release; distribution is unlimited.		
17. DISTRIBUTION STATEMENT (of the abstract entered in Block 20, if different from Report)		
18. SUPPLEMENTARY NOTES  W. J. Kolkert of the Prins Maurits Laboratorium TNO, The Netherlands, served as a Special Project Officer at ARDC.		
19. KEY WORDS (Continue on reverse side if necessary and identify by block number) Deceleration                      Railgun Magnetic field                      Flux compression Field diffusion                      Joule heating Induction                      Liner Sliding contacts                      Theta current		
20. ABSTRACT (Continue on reverse side if necessary and identify by block number)  A simple model for the electromagnetic deceleration of a moving metallic projectile is described. This model incorporates the influence of magnetic field parameters, time-dependent field diffusion, and device geometry to approximate the braking action. The model predicts that a viable experi- mental braking device can be designed.		

# CONTENTS

	Page
Introduction	1
Modeling of Braking Action	1
Calculated Results	4
Discussion	5
Conclusions	6
References	7
Distribution List	13

**DTIC**  
**ELECTE**  
**S** **D**  
**JAN 15 1985**  
**B**

Accession For	
NTIS GRA&I	<input checked="" type="checkbox"/>
DTIC TAB	<input type="checkbox"/>
Unannounced	<input type="checkbox"/>
Justification	
By	
Distribution/	
Availability Codes	
Dist	Avail and/or Special
A-1	

DTIC  
 COPY  
 INSPECTION

## INTRODUCTION

It has long been known that solid objects (e.g. projectiles) can be accelerated by electromagnetic (EM) forces (ref 1). Typically, currents are required to flow either in the projectile or in an arc behind it. These currents can be supplied through sliding contacts, induced during the acceleration process, or pre-established (persistent) (ref 2).

Deceleration of a moving projectile is possible by operating an EM acceleration system in the reverse mode. Such schemes involve a degree of flux compression such as that incorporated in the inverse railgun concept recently espoused by Marshall (ref 3), which accomplishes projectile deceleration as a means of transferring electrical energy to a separate load.

The subject of this report is the passive electromagnetic braking of a moving projectile where kinetic energy is directly converted into heat. The phenomenon has an intrinsic conceptual appeal, and potential applications include the controlled "soft" catch of appropriately configured projectiles in flight.

A simple model was conceived to obtain some feeling for the magnitude of parameters involved in the electromagnetic braking process and constraints imposed upon the design of a braking device. The model considers the motion of a cylindrical, metallic projectile in an axial magnetic field uniformly distributed in a space confined by a fixed, resistive, cylindrical liner which is coaxial with the moving projectile.

Field compression in the gap between the moving projectile and the liner causes  $\theta$ -currents to rise along the projectile surface and the adjacent segment of the liner surface by field diffusion in both conducting materials. These currents give rise to resistive Joule heating caused by the time dependence of field diffusion and the motion of the projectile. The induced currents, especially in the liner, show a nonuniform distribution in the relatively short time interval during which the projectile moves along its own length. The net force resulting from the interacting current distributions on the projectile and the adjacent liner segment is anticipated to be nonvanishing and will counteract the projectile's motion. In this way, the projectile is losing its kinetic energy while at the same time, resistive Joule heating is generated in the projectile and the liner.

## MODELING OF BRAKING ACTION

The model described is illustrated in figure 1. A cylindrical metallic projectile with mass  $m_p$ , radius  $r_0$ , length  $L_p$ , conductivity  $\sigma_p$ , and permeability  $\mu_p$  moves with velocity  $v$  in an axial uniform magnetic field  $B_0$ . The space is confined by a fixed resistive liner with inner and outer radii  $r_1$  and  $r_2$ , respectively, conductivity  $\sigma_L$ , and permeability  $\mu_L$  (fig. 1).

The field is assumed to be compressed discontinuously in the gap between the projectile surface and the adjacent liner surface (radii  $r_0$  and  $r_1$ , respectively) at axial positions  $z_1$  and  $z_2$ .

The motion of the projectile is hypothesized to be such that magnetic energy is conserved throughout the braking process. Neglecting mechanical work associated with nonaxial forces on components, conservation of energy gives

$$m_p v \frac{\delta v}{\delta t} = - \frac{\delta H}{\delta t} \quad (1)$$

where  $H$  is the resistive Joule heating generated in the projectile and the liner during braking.

The magnetic field in the gap between the projectile and the liner is of induction

$$B_z = B_0 \left[ \frac{r_1^2}{r_1^2 - r_0^2} \right] \quad (2)$$

for  $r_0 < r < r_1$  and  $z_1 < z < z_2$ .

It is assumed that  $B_z$  is a constant during the braking process and that its value is independent of the location on the surfaces of bordering projectile and liner.

For radial diffusion of the magnetic field in the liner segment adjacent to the moving projectile, the equation (ref 4)

$$\frac{\delta^2 \hat{B}_z}{\delta r^2} - \mu_L \sigma_L \frac{\delta \hat{B}_z}{\delta t} = 0 \quad (3)$$

where

$$\hat{B}_z(t = 0) = 0 \text{ and } \hat{B}_z = B_z - B_0$$

is valid.

Equation 3 leads to

$$\hat{B}_z = \hat{B}_z(r_1) \left[ 1 - \frac{2}{\sqrt{\pi}} \int_0^{\sqrt{\frac{\mu_L \sigma_L}{4t} (r-r_1)}} e^{-\omega^2} d\omega \right] \quad (4)$$

The induced  $\theta$ -currents in the liner are given by

$$J_L = -\frac{1}{\mu_L} \frac{\partial B_z}{\partial r} \quad (5)$$

Equations 4 and 5 give;

$$J_L = \frac{B_z(r_1)}{\mu_L} \sqrt{\frac{\mu_L \sigma_L}{\pi t}} e^{-\frac{\mu_L \sigma_L}{4t} (r-r_1)^2} \quad (6)$$

Similar results are obtained for the induced currents in the projectile where  $B_z$  is the magnetic field at the conductor surface. The heat generated per unit time,  $\frac{\delta H}{\delta t}$ , in the conducting surfaces of projectile and liner bordering the gap between them, is expressed by:

$$\frac{\delta H}{\delta t} = \int_{z_1}^{z_2} \left[ \frac{2\pi r_1}{\sigma_L} \int_{r_1}^{\infty} J_L^2 dr + \frac{2\pi r_o}{\sigma_p} \int_{-\infty}^{r_o} J_p^2 dr \right] dz \quad (7)$$

where  $J_L$  and  $J_p$  are the currents induced in the liner and projectile, respectively, and where  $z_2 - z_1 = L_p$ .

Equation 7 leads to

$$\frac{\delta H}{\delta t} = \frac{2\pi r_1}{\sigma_L} \left[ \frac{B_z(r_1)}{\mu_L} \right]^2 \int_{z_1}^{z_2} \sqrt{\frac{\mu_L \sigma_L}{2\pi t}} dz + \frac{2\pi r_o}{\sigma_p} \left[ \frac{B_z(r_o)}{\mu_p} \right]^2 L_p \sqrt{\frac{\mu_p \sigma_p}{2\pi t}} \quad (8)$$

In performing the integration over  $z$  in equation 8, the time scale in the liner segment covered by the moving projectile is running from zero to  $L_p/v$ , while the time scale for the generation in the projectile is running from the beginning towards the end of the braking process (accumulation). The dynamics mentioned here cause the nonuniform distribution of  $\theta$ -currents (eq 6) in the liner segment adjacent to the moving projectile and are the source for a net braking force on the projectile.

Combining equations 1 and 8 gives the analytical expression

$$m_p v \frac{\delta v}{\delta t} = - \left[ \beta_L v^{1/2} + \beta_p t^{-1/2} \right] \quad (9)$$

describing the braking action in the chosen setup.

In equation 9,  $\beta_L$  and  $\beta_p$  are

$$\beta_L = \frac{2\pi r_1}{\sigma_L} \left[ \frac{B_z(r_1)}{\mu_L} \right]^2 \sqrt{\frac{2\mu_L \sigma_L L_p}{\pi}} \quad (10)$$

$$\beta_p = \frac{2\pi r_o}{\sigma_p} \left[ \frac{B_z(r_o)}{\mu_p} \right]^2 L_p \sqrt{\frac{\mu_p \sigma_p}{2\pi}}$$

### CALCULATED RESULTS

To obtain some feeling for the magnitude of parameters involved in electromagnetic braking, an example involving the motion of a cylindrical steel projectile in an axial magnetic field in a space confined by a copper liner (fig. 1) is analyzed. Solving equation 9 numerically with a steel projectile mass  $m_p = 6$  kg, length  $L_p = 0.508$  m, radius  $r_o = 0.0508$  m,  $\mu_p = 2 \times 10^{-4}$  Wb/A m,  $\sigma_p = 0.38 \times 10^7$  mho/m, and a copper liner with radius  $r_1 = 0.05334$  m,  $\mu_L = 12.57 \times 10^{-7}$  Wb/A m, and  $\sigma_L = 5.8 \times 10^7$  mho/m gives the data of table 1 when braking action starts at a projectile velocity  $v_o = 600$  m/s.

The length,  $\Delta L$ , and time,  $\Delta t$ , involved in braking the projectile to a final velocity of zero m/s and the overall heat generated in the liner,  $\Delta H_L$ , and the projectile,  $\Delta H_p$ , are given in table 1.  $\Delta L$  and  $\Delta t$  are calculated with equation 9 ( $V, t$  - history), and  $\Delta H_L$  and  $\Delta H_p$  are calculated with equation 10.

Table 1. Electromagnetic braking action parameters for a steel projectile and copper liner

Magnetic field, $B_o$ (T)	Length, $\Delta L$ (m)	Time, $\Delta t$ (s)	Liner heat, $\Delta H_L$ (J)	Projectile heat, $\Delta H_p$ (J)
1	12.9	$34.5 \times 10^{-3}$	$1.079 \times 10^6$	504
2	3.1	$8.7 \times 10^{-3}$	$1.079 \times 10^6$	$1.01 \times 10^3$
3	1.4	$3.9 \times 10^{-3}$	$1.078 \times 10^6$	$1.5 \times 10^3$



Keeping other parameters constant, the influence of gap-width ( $r_1 - r_0$ ) on braking length,  $\Delta L$ , time,  $\Delta t$ , and heat generated in the projectile,  $\Delta H_p$ , is shown in figures 2, 3, and 4, respectively.

If other materials for projectile and liner are considered (e.g., changing only  $\mu$  and  $\sigma$  with respect to values mentioned above), substantial changes in braking length and time are calculated. If, for example, a tungsten projectile and copper liner are taken, braking lengths and times are reduced by a factor of about 2 to 3 and heat generated in the projectile is increased by a factor of about 1000. Taking a steel liner and a steel or tungsten projectile increases braking lengths to many tens of meters and times to many seconds.

Although not indicated here numerically, the influence of projectile mass on braking length and time appears to be almost proportional.

## DISCUSSION

The model presented here contains a number of limitations. For instance, a practical device for electromagnetic braking of a metallic projectile would have a finite length. Braking the motion of the projectile on entering the magnetic field, present in the setup depicted in figure 1, is substantial and is not modeled here. During compression of the magnetic field in the gap between the moving projectile and the liner, the change in magnetic induction is continuous [not discontinuous as assumed here (fig. 1)] and slightly different at the front and the rear of the projectile. Although current distributions on liner and projectile surfaces will then be more complicated, as will force distributions, it is not anticipated that calculated results will change drastically (i.e., not more than a factor of two).

A more substantial limitation of the model is the assumption that  $B_z$  (magnetic induction) in the gap is a constant during braking. As a result of diffusion of the B-field in the projectile and adjacent liner surfaces,  $B_z$  on these surfaces will change not only in going from  $z_1$  toward  $z_2$  (fig. 1) but also during the whole braking process. Leakage of the compressed field from the gap causes less braking action than calculated. However, depending on the magnitude, the braking time,  $\Delta t$ , leakage will have a minor influence on calculated parameters when the associated skin depth [ $\delta$  ( $\delta = \pi \Delta t / (\mu \sigma)$ )] is smaller than the gap width ( $r_1 - r_0$ ) considered. Application of the model presented here implies, therefore, that braking times in the order of a few milliseconds or less have to be considered. In addition, the effectiveness of the model may be further enhanced by restricting attention to ferromagnetic projectiles. Apart from the limitations mentioned above, the calculated results show that with realistic values for initial magnetic induction and gap width, metallic projectiles with a mass and initial velocity of interest can be decelerated over an acceptable length.

In designing a device, the mechanical strength constraints related to the construction of the projectile to be decelerated, the liner and the B-field generating coil have to be considered. In the gap between the moving projectile and

the adjacent liner segment, mechanical stresses on both materials can rise as high as 4 to 8 kbar with  $B_0$  and  $(r_1 - r_0)$  values of several tesla and mm, respectively. Temperature rises in the projectile and liner surface layers caused by resistive Joule heating are minor for the  $B_0$  and  $(r_1 - r_0)$  values.

### CONCLUSIONS

Within the constraints of the model, calculated results showed that with values for the magnetic induction  $B_0$  of several tesla and a gap width between projectile and liner of several mm's, a steel projectile with a mass of 6 kg and an initial velocity of 600 m/s can be slowed down to rest over a length of several meters without excessive stress-loading or heating of components.

## REFERENCES

1. 1980 Conference on Electromagnetic Guns and Launchers, IEEE, Trans. on Magnetics, vol 18, 1982, pp 3-216.
2. T. Gora and P. J. Kemmey, IEEE, Trans. on Magnetics, vol 19, 1983, p 1569.
3. R. A. Marshall, Second Symposium on Electromagnetic Launch Technology, Boston, MA, 10 - 13 October 1983, p 27.
4. J. D. Jackson, Classical Electrodynamics, second edition, J. Wiley and Sons, New York, NY, 1975.

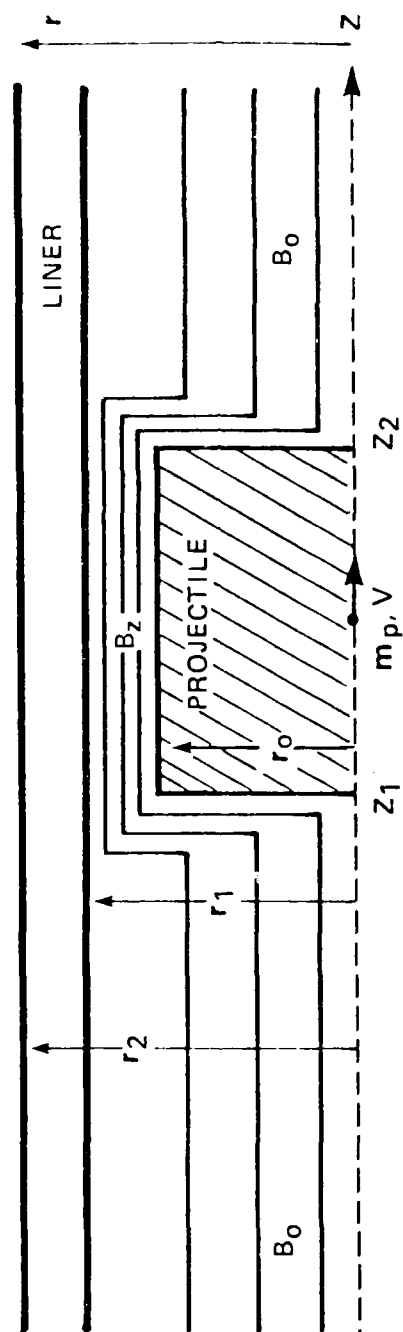


Figure 1. Magnetic field configuration around a metallic projectile moving in an axial field confined by a resistive liner (axis-symmetric part is shown)

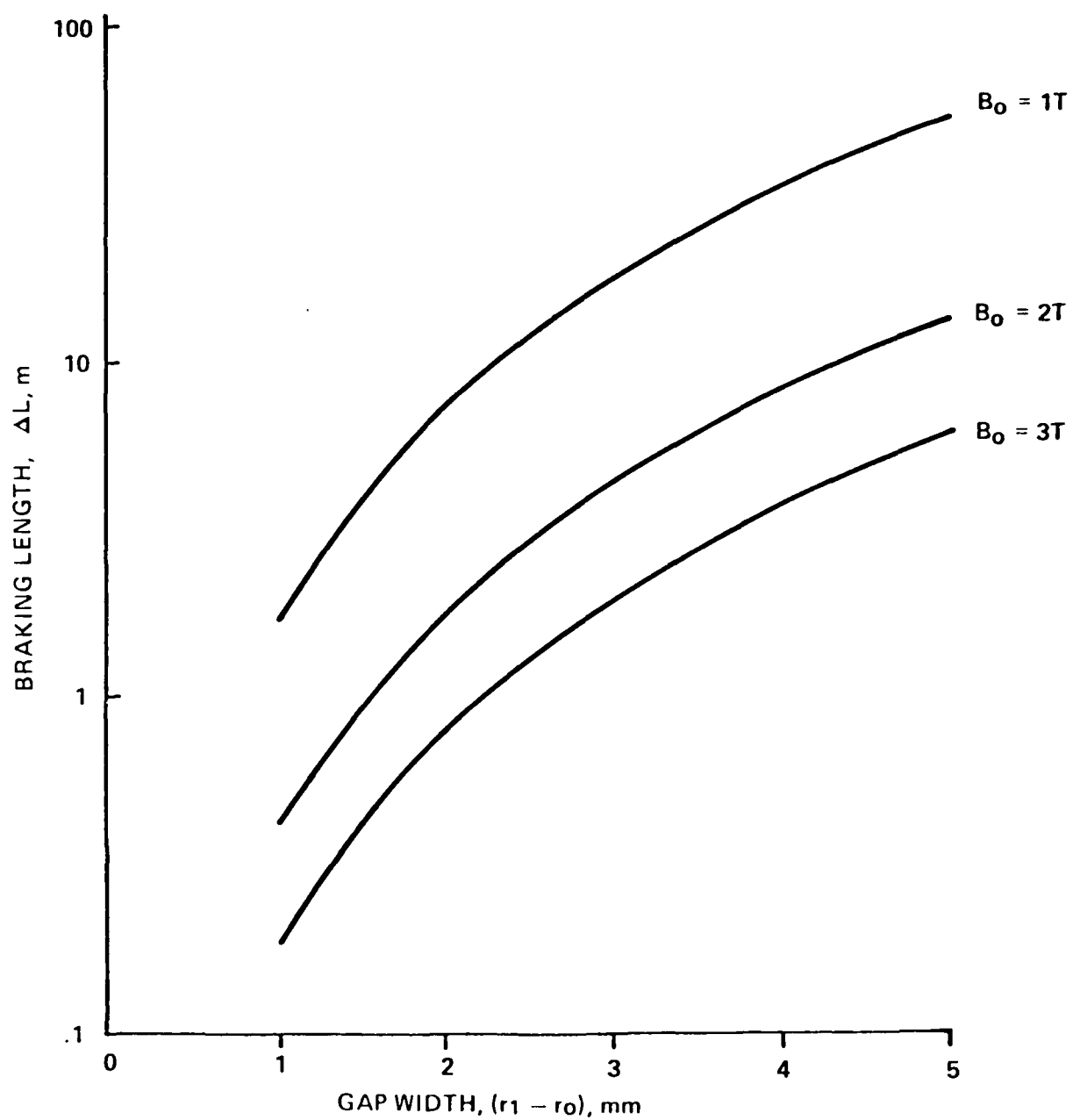


Figure 2. Braking length  $\Delta L$  as a function of gap-width for a steel projectile and copper liner,  $B_0 = 1, 2$ , and  $3T$ .

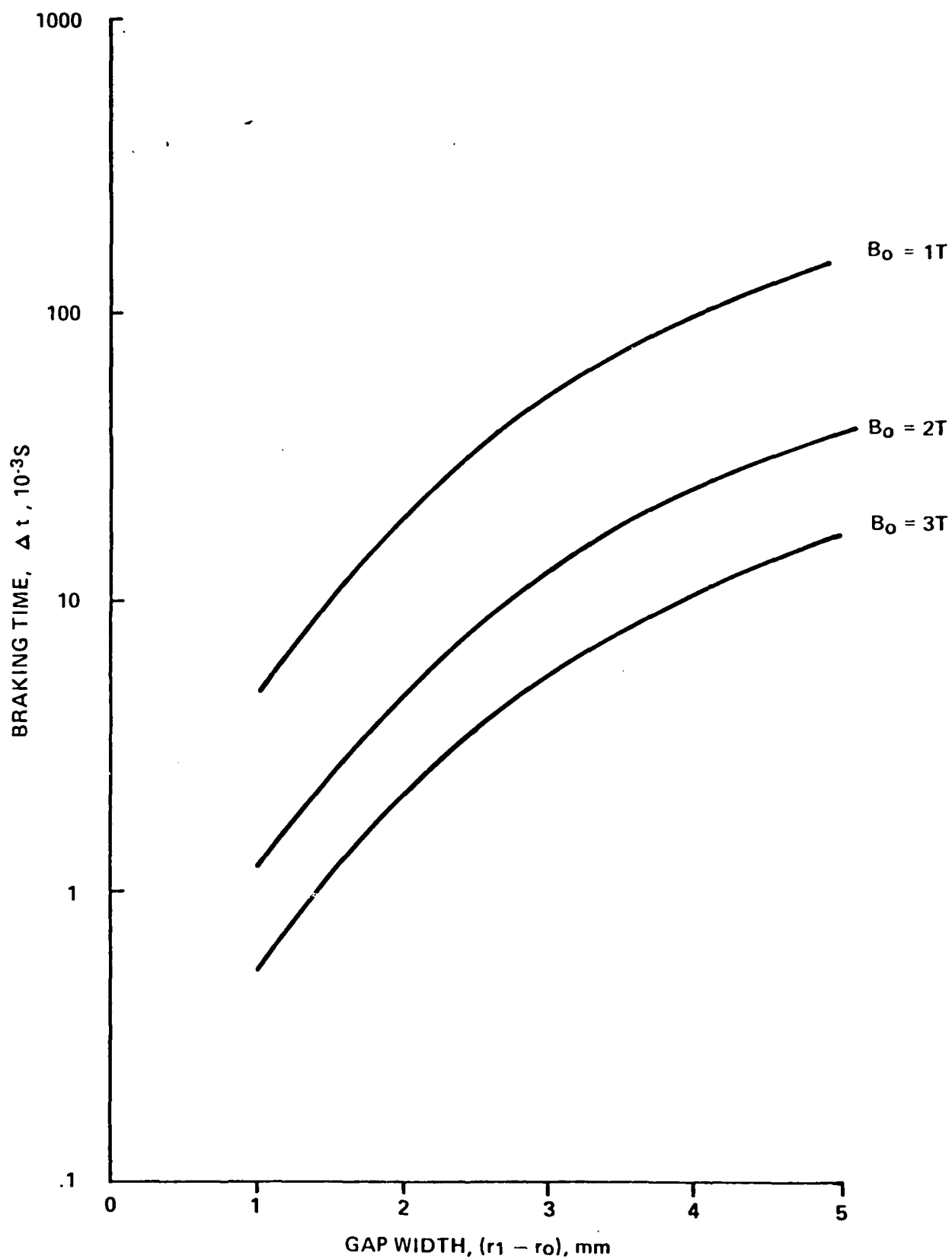


Figure 3. Braking time  $\Delta t$  as a function of gap-width for a steel projectile and copper liner,  $B_0 = 1, 2$ , and  $3T$

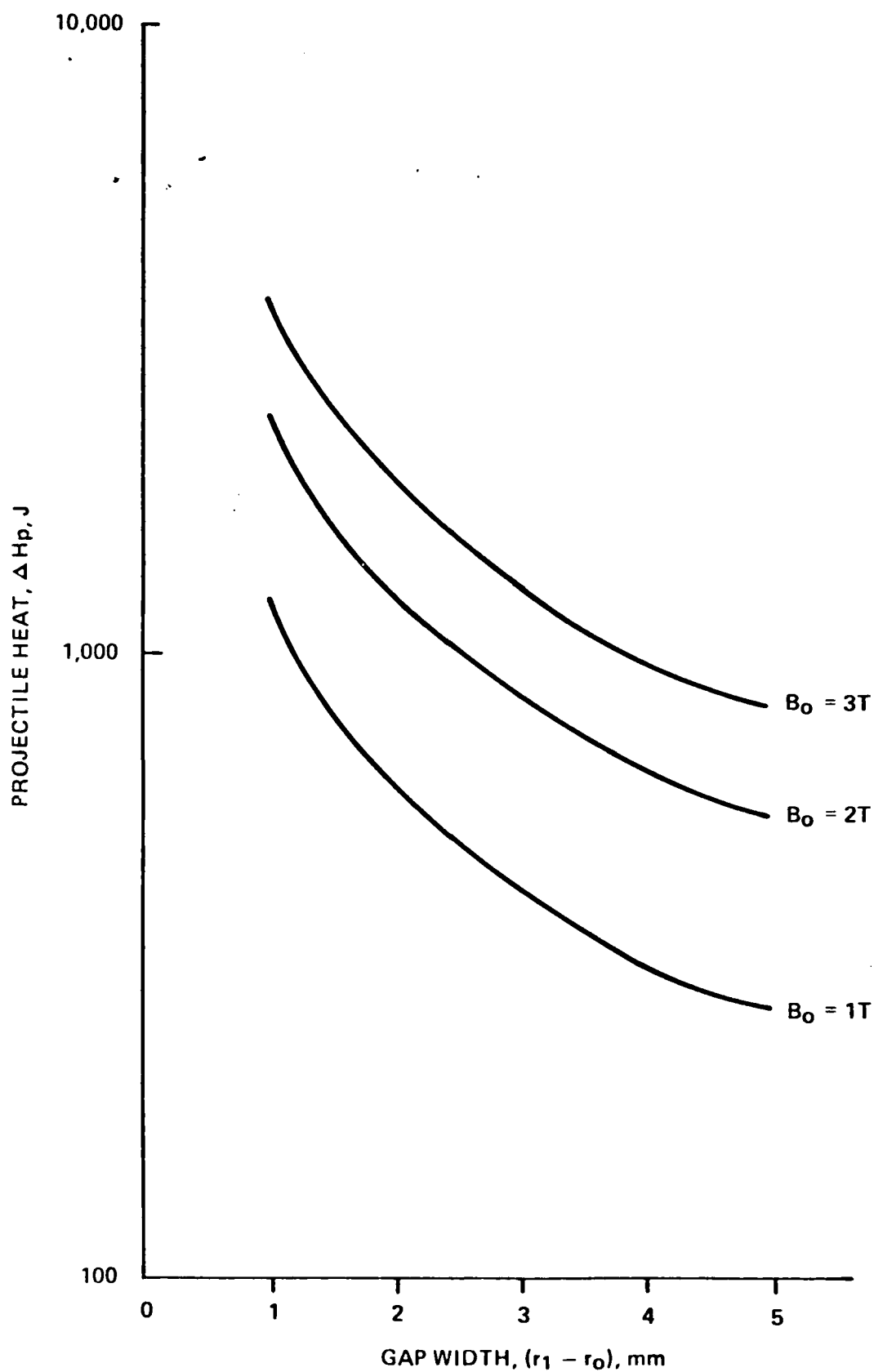


Figure 4. Projectile heat  $\Delta H_p$  generated during braking as a function of gap-width for a steel projectile and copper liner,  $B_0 = 1, 2$ , and  $3T$

## DISTRIBUTION LIST

### Commander

Armament Research and Development Center  
U.S. Army Armament, Munitions and Chemical Command  
ATTN: SMCAR-LCA-G (5)  
SMCAR-TSS (5)  
SMCAR-SF  
Dover, NJ 07801-5001

### Commander

U.S. Army Armament, Munitions and Chemical Command  
ATTN: AMSMC-GCL(D)  
AMSMC-QAR-R(D)  
Dover, NJ 07801-5001

### Administrator

Defense Technical Information Center  
ATTN: Accessions Division (12)  
Cameron Station  
Alexandria, VA 22314

### Director

U.S. Army Materiel Systems Analysis Activity  
ATTN: DRXSY-MP  
Aberdeen Proving Ground, MD 21005-5066

### Commander/Director

Chemical Research and Development Center  
U.S. Army Armament, Munitions and Chemical Command  
ATTN: SMCCR-SPS-I  
SMCCR-RSP-A  
APG, Edgewood Area, MD 21010-5423

### Director

Ballistic Research Laboratory  
ATTN: AMXBR-OD-ST  
Aberdeen Proving Ground, MD 21005-5066

### Chief

Benet Weapons Laboratory, LCWSL  
Armament Research and Development Center  
U.S. Army Armament, Munitions and Chemical Command  
ATTN: SMCAR-LCB-TL  
Watervliet, NY 12189-5000

### Commander

U.S. Army Armament, Munitions and Chemical Command  
ATTN: AMSMC-LEP-L  
Rock Island, IL 61299-6000



Director  
U.S. Army TRADOC Systems  
Analysis Activity  
ATTN: ATAA-SL  
White Sands Missile Range, NM 88002

Director  
Defense Advanced Research Projects Agency  
ATTN: DARPA-TTO, H. D. Fair, Jr.  
1400 Wilson Boulevard  
Arlington, VA 22317

Commander  
Ballistic Missile Defense System Command  
ATTN: BMD/ATC-M, Darrell Harmon  
P.O. Box 1500  
Huntsville, AL 35807

Center of Electromechanics  
ATTN: W. Weldon  
Taylor Hall 227  
University of Texas at Austin  
Austin, TX 78712

Commander  
HQ, AFSC/DLWA  
ATTN: CPT R. Reynolds  
Andrews Air Force Base, MD 20334

Commander  
Naval Sea Systems Command  
ATTN: LCDR, Joseph R. Costa  
Washington, DC 20362

Commander  
Air Force Armament Technology Laboratory  
ATTN: DLDG, Timothy Aden  
Eglin Air Force Base, FL 32542